2020 IEEE/RSJ International Conference on Intelligent Robots and Systems (IROS)
October 25-29, 2020, Las Vegas, NV, USA (Virtual)

Model Identification of a Soft Robotic Neck

Fernando Quevedo*, Jorge Muñoz Yañez-Barnuevo, Juan A. Castano, Concepción A. Monje, Carlos Balaguer.

***Abstract*— Soft links and actuators are nowadays emerging technologies aiming to overcome some problems in robotics such as weight, cost or human interaction. However, the nonlinear nature of their elements can make their characterization challenging and hinder the use of standard control engineering tools. In this paper, we explore different state-of-the-art identification methods for the soft neck, in order to find a reliable plant model. Even though the neck has three Degrees of freedom, in this work we only consider the planar deflection of the link as a starting point for future analysis. Given the nonlinear nature of the soft neck, we consider two identification strategies, i.e., set membership, which is a data driven, nonlinear and nonparametric identification strategy, and Recursive Least Squares at selected linearization points. A neural network identification is also given for comparison purposes. Results show that the explored methods offer a suitable alternative to identify the dynamics of the neck that allows their implementation for simulation and future control.**

I. Introduction

Soft robotics is a new field of research in robotics. Due to their intrinsic properties of compliance and adaptability, these technologies could improve many of current robotics problems, such as weight, cost, and human interaction. Many new prototypes with soft technologies have begun to emerge in recent years using different actuator technologies: pneumatic [1]–[3], super memory alloys (SMA) [4], tendon based [5], [6]. But these new technologies still come with their own drawbacks. Kinematic models, unlike rigid robotics, are not yet well understood. Numerous simplifications or assumptions are made to control and actuate them, making them not as reliable as their rigid counterparts, thus limiting their impact on robotics [7]. Meanwhile, in other research fields such as rehabilitation, where precision is not as important, these technologies are thriving [4], [8].

Nonetheless, improvements could be made to reduce energy consumption and force requirements. One of the most commonly overlooked components for soft robotics are passive gravity compensation mechanisms [9]. The aforementioned mechanism can greatly reduce the energy used by the systems. This is accomplished thanks to their ability to store the energy as internal deformations. Also, at the same time, they mitigate the force of gravity.

In [2] a globe with pneumatic bending actuators is proposed. In that system, the deformations of the actuators chamber surface were approximated with finite element models (FEM). In their simplifications, the authors consider only slow movement of the system in a 2-dimensional space. Therefore, the dynamic energy was neglected from the model. In [3] a 2-dimensional model of a soft fluidic actuator was studied with two different techniques, one geometrical and one FEM. The geometrical model was created with a simplification of uniform bending curvature. Geometric models, in their results, showed similar trends to the experimental data, while the FEM model resulted in linear trends. A 3 dimensional model for a pneumatic soft arm was presented in [10]. In that work the effects of gravity were denied and no payload was considered. In addition, the authors considered a constant curvature on the bending segments. ExtenSA soft limb, [1], approached the model with a geometric perspective, neglecting the effects of gravity or internal elastic forces.

Tendon based actuators are mainly used for exoskeletons. In the hand exoskeleton in [5], [6], a 3-link kinematic chain model is proposed for each finger. In both kinematics, all joints are considered to be pure revolute joints. Also, the friction caused by the cable guides is neglected and no deformations occur due to forces inside the cable guides.

A different approach for identification of kinematics is given by [11] were a black box identification of a fluidic actuator was presented. Using this method, the model includes the shear deformation of the model, which was ignored in previous models. The identification was done with the Matlab Identification toolbox, with a second order transfer function for different frequencies that resulted in high uncertainty, the maximum parametric variations reaching 36%, that needed to be compensated by a backstepping controller.

This work aims to characterize a soft neck described in [12], which is an improved version of the initial proposal [13]. The new neck system features a soft material link that replaces the original spring, resulting in a lighter and more robust system. In addition, a tilt sensor has been set on the tip, which allows inclination and orientation sensing, and feedback control.

Although the original spring system was already nonlinear as seen in [13], the new material adds additional nonlinearity. The resulting theoretical model is outside the standard modeling methods. As a consequence, a nonlinear identification has been considered for the system, in order to have a model for simulation and control. Furthermore, linear identification will be used at several specified equilibrium points for comparison.

Some identification has been done in [12] for control design, but it was limited to actuators and ignored the dynamics of the link. In our work we use two identification methods for the whole plant, including the actuators and the soft link. To simplify, we only consider the tip inclination as

*All authors are with the Systems Engineering and Automation Dpt., University Carlos III of Madrid, Leganes, Madrid, Spain. fquevedo, jmyanezb, jucastan, cmonje, balaguer @ing.uc3m.es

978-1-7281-6211-9/20/$31.00 ©2020 IEEE

system output.

Finally, the soft neck is installed in the robot TEO [14], a full size humanoid developed in the facilities of the Robotics Lab at Carlos III university of Madrid. The hardware design has been updated since [12] to get a more compact system, suitable for the robot. For this approach, motors have been replaced for smaller alternatives, resulting in the current design described below.

II. Soft Neck Description

The main part of the soft neck is the soft link that acts as the spine. It is a central bendable soft link and a parallel mechanism driven by cables, which produces a tilt in the upper platform. Any inclination and orientation can be achieved by just configuring the right lengths of the tendons. Fig. 1 shows the soft neck prototype and its parts.

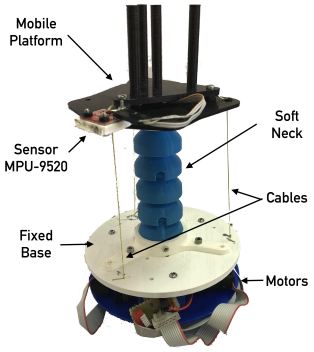

Fig. 1: Soft neck platform

The neck is composed of a base, a mobile platform, the mechanical soft link, tendons and motors, as Fig. 1 shows. All parts were built with a 3D printer, including the soft link, with a weight of $100g$ (excluding motors and hardware).

Tendon lengths are established using the three actuators located at the base, each with motor, gear, encoder and driver with the following characteristics:

- Driver: Technosoft iPOS4808 MX-CAN; 400 W, 12-50 Volt, 8 Amp (intelligent motor driver)
- Motor: Maxon RE 16-118739; graphite brushes, 48 Volt, 4 Watt
- Gear: Maxon 134777 (24 : 1)
- Encoder: Maxon mr201937

By setting different tendon lengths, the neck can show any inclination and orientation as defined in Fig. 2, but only the inclination is considered for our purposes, therefore, only one actuator is used as the system input. With this scheme, the inverse kinematics described in [15] is not necessary, which makes identification easier. Subsequently, results can be generalized by applying these identification methods for the Multiple Inputs Multiple Outputs (MIMO) case. Even though there may be geometrical relations, those might not be straightforward or possible to obtain.

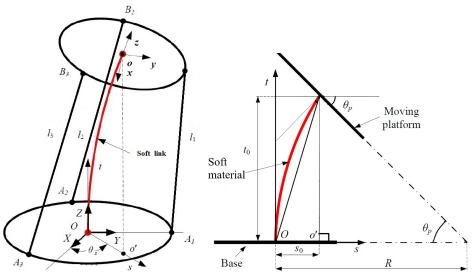

Fig. 2: Soft neck kinematics. Orientation and inclination variables [13] .

The actuator position and velocity low level control is managed by the iPos © Intelligent drives, therefore there is no motor control apart from the driver internal control. Some loops have been used for identification purposes, but all system data has been captured as an open-loop plant, with actuator velocity as input and inclination (θ, $\Delta\theta/\Delta t$) as output.

Since the inclination sensor is considered as output, the resulting model will describe the inclination as a function of the motor input. As the main source of nonlinearity is the central link, and more specifically, the bend angle, we expect to find a different plant response depending on the inclination. For this reason, the actuator velocity is a good choice for system identification: it has a zero mean for any constant motor position, and a meaningful system output is the inclination speed (tilt time derivative).

Two different methods of system identification are used. First, set membership method as described in [16] is used for nonlinear identification, and second, recursive least squares (RLS) as described in [17] is applied for different tilt configurations, which will result in a linear system for each RLS identification performed. The evolution of these systems, according to the inclination, will be studied.

Both methods are briefly described in sections III and IV, followed by a description of the experimental setup and experiments. Finally, results are shown and discussed.

III. Set Membership Identification

In this section, we briefly describe the nonlinear Set-Membership identification method as in [16].

A system whose structure is NARX (Nonlinear AutoRegressive with eXogenous input) can described as

$$y(t) = f_o(w(t)) \tag{1}$$

where

$$w(t) = [y(t-1), \ldots, y(t-n_y), u(t), \ldots, u(t-n_u)],$$
$$w(t) \in \mathcal{R}^n, n = n_y + n_u$$

A SISO (Single Input-Single Output) system is assumed without loss of generality.

Although the function f_o is unknown, a set of measurements $\widetilde{y}, w$ of y and w is available. The objective is to find an estimate $\hat{f}$ for f_o.

For this purpose, the measurements

$$\widetilde{y}(k) = f_o(\widetilde{w}(k)) + e(k) \tag{2}$$

for $k = 1, 2, \ldots, N$. Where $e(k)$ is the measurement error and $|e(k)| \leq \epsilon$.

The following information on f_o is available

$$f_o \in \mathcal{F} \doteq \left\{ f \in C^1(W) : \|f'\| \leq \gamma, \forall w \in W \right\} \tag{3}$$

where $f'(w)$ denotes the gradient of $f(w)$ and $\|x\|$ is the Euclidean norm.

Hence, the Feasible System Set (**FSS**) of the system is:

$$FSS \doteq \{ f \in \mathcal{F} : |\widetilde{y}(k) - f(\widetilde{w}(k))| \leq \epsilon, k = 1, 2, \ldots, N \} \tag{4}$$

This set consists of all the functions in $\mathcal{F}$, consistent with prior information and measurements.

If prior assumptions are true, $FSS \neq \emptyset$ and $f_o \in FSS$. Hereinafter, prior hypotheses are assumed to be valid.

The optimal estimate for $f_o(w)$ is given by

$$f_c(w) \doteq \frac{f_u(w) + f_l(w)}{2} \tag{5}$$

$$f_u(w) = min_{1 \leq k \leq N}(\widetilde{y}(k) + \gamma \|w - \widetilde{w}(k)\|) \tag{6}$$

$$f_l(w) = max_{1 \leq k \leq N}(\widetilde{y}(k) - \gamma \|w - \widetilde{w}(k)\|) \tag{7}$$

From theorems 2, 5 and 7 in [16], it follows that

- $f_u(w)$ and $f_l(w)$ are optimal bounds for $f_o(w)$;
- $f_u(w)$ and $f_l(w)$ are Lipschitz continuous on W;
- f_c is optimal for any $L_p(W)$ norm, with $p \in [1, \infty]$;

where the optimality criterion is:

$$f_{opt} = \arg\inf_{\hat{f}} \sup_{f \in FSS} \left\| f - \hat{f} \right\|_p$$

Given the model complexity of the method [18], different approaches were proposed to reduce the identification time [19], [20] and facilitate its implementation in fast applications. However, this is not part of our work here.

A. Set Membership Identification Procedure

To implement the identification of the Set membership Nearest point, it is first necessary to generate and informative data set that covers the entire working space of the neck. For this purpose we implemented a sinusoidal sum with different frequencies to cover the workspace. This signal was applied in velocity to the neck which is being controlled in open loop and we sensed the position, velocity and inclination of the neck to generate enough informative data.

Afterwards, it is necessary to identify the size of the regressor. We implemented different neural networks to obtain the regresor with the best fit over the identification data set. Using position and velocity as input regressor and neck inclination as output, we obtained the validation for Normalized Root Mean Square Error ($NRMSE$) data set of a 92% adjustment when using the regressor:

$$w(t) = [y(t-1), ..., y(t-3), u1(t-8), ..., u1(t-10), \\ u2(t-8), ..., u2(t-10), u3(t-8), ..., u3(t-10)]$$

using as hypothesis for the Set membership $\delta = 0.5$, $\epsilon = 0.01$ which were validated in the data set.

IV. Recursive Least Squares Identification

It is not possible to use a linear method in our non-linear plant, but using a linear approximation is possible within a small region around an operating point. Therefore, defining several points inside the inclination range and performing RLS identification can provide with one linear model for each operating point if parameter convergence is achieved. Once the parameters are obtained, their values can be examined in order to get a parameterized transfer function, that is, an adjustable linear model depending on inclination.

The discrete domain SISO model of the proposed system can be described by the following ARX structure (auto-regressive with exogenous terms) equation:

$$y(t) = -a_1 y(t-1) - .. - a_{na} y(t-na) + \\ b_1 u(t-1) + .. + b_{nb} u(t-nb), \tag{8}$$

where $y(t)$ and $u(t)$ are plant output and input variables at time t, and can be expressed as a matrix as:

$$y(t) = \theta \phi'(t-1), \tag{9}$$

where $\theta = [a_1, .., a_{na}, b_1, .., b_{nb}]$ and $\phi(t-1) = [-y(t-1), .., -y(t-na), u(t-1), .., u(t-nb)]$.

Equation (9) represents a model output prediction based on past inputs and outputs ($\phi(t-1)$), and model parameters (θ). Recursive identification methods use Eq. (9) as a predictor for the next system output just advancing the index one position ($\hat{y}(t+1) = \hat{\theta}(t)\phi'(t)$). Based on current model estimate $\hat{\theta}$, and real (y) system output, prediction error is:

$$\epsilon(t) = y(t) - \hat{y}(t) \Rightarrow \epsilon(t+1) = y(t+1) - \hat{y}(t+1). \tag{10}$$

When the next data $y(t+1)$ is available, it is used in error reduction by providing a fitter $\hat{\theta}(t+1)$, and therefore a better plant estimate. How the error is reduced depends on the identification method. Recursive least squares use the squared error of all previous data. At this point, the RLS method is only applicable to linear time invariant (LTI) systems, because all past identification data are considered, and system variations are not tracked, but integrated into the same model.

Therefore, as our plant parameters are expected to change depending on inclination, the adapted method described in [17] as RLS with constant forgetting factor (CFF-RLS) is more suitable. This method introduces λ, a parameter changing the impact of past identification data known as forgetting factor. Constant forgetting factor RLS is summarized in the following equations:

$$\hat{\theta}(t+1) = \hat{\theta}(t) + F(t+1)\phi(t)\epsilon(t+1), \tag{11}$$

$$\lambda F(t+1) = F(t) - \frac{F(t)\phi'(t)\phi(t)F(t)}{\lambda + \phi(t)F(t)\phi'(t)}, \tag{12}$$

$$\epsilon(t+1) = y(t+1) - \hat{\theta}(t)\phi'(t). \tag{13}$$

This algorithm is based on known input and output data $\phi(t)$, the immediate previous model estimate $\hat{\theta}(t)$ and the prediction error $\epsilon(t+1)$, according to Eq. (10). When $\lambda = 1$, the RLS method is obtained, using all past values. The forgetting factor requires $\lambda < 1$, where the smaller λ, the higher preference for current values (stronger forgetting factor). See [17] or [21] for a more detailed discussion about RLS and other identification methods. As advised in the literature, we used $\lambda = 0.98$ as a compromise between model update and parameter stability.

V. Experimental Setup

As the objective of this work is the soft link identification for control purposes, it can be done offline, and the open loop identification is enough to obtain a valid plant model that we can use. Note that open loop identification can be done within a feedback loop if proper data filtering is performed (see [22]). In this sense, a set of experiments has been designed for data capture.

As stated before, only the planar case is considered for link deflection, therefore, only one tendon needs actuation. There is a direct correspondence between motor position and tendon length, therefore, the angular motor variables are considered as inputs, while measured sensor inclinations are used as system outputs. Data capture involves the following inputs and outputs:

- Motor input position (rad)
- Motor input velocity ($\frac{rad}{s}$)
- Platform inclination or model output (^{o})

Specific data capture was used for each previously described method in order to find a model. Then, a common data set has been used for method comparison.

A. Maximum response frequency

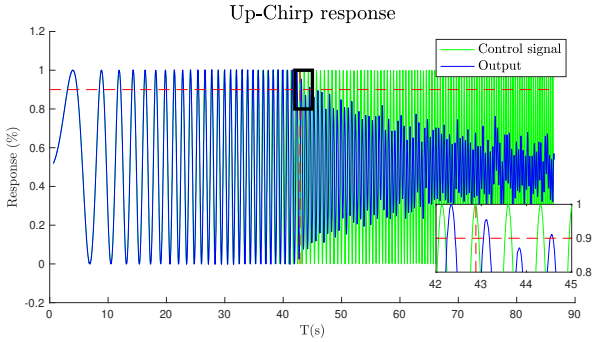

Fig. 3: System response to Chirp wave.

To identify the model, the maximum response frequency must be determined. An up-Chirp wave, which consists in a sine wave with a frequency that increases with time, has been used to establish the frequency. Once the system responds to the control signal with less than 90% amplitude, the frequency is reached as shown in Fig. 3. The up-chirp signal selected responds to the equations 14 and 15 where CS is the control signal, f is frequency and t is time.

$$CS = 5 + 4 * sin(f * t) \tag{14}$$

$$f = t * 0.1 \tag{15}$$

The final identified frequency was 4.2 $\frac{rad}{s}$ which was rounded to $4\frac{rad}{s}$, to guarantee the system responsiveness.

B. Data set capture

The system motion must include some features to capture all its dynamics. Although some works such as [23] have managed to avoid the use of system persistent excitation signals in closed loop systems, there is no reason to avoid this use in the open loop offline identifications as proposed here. Therefore, a pseudo-random signal along with the reference input is used here, as described in [17], to obtain enough system information in the data sets.

Neck actuator motion was programmed to follow a composition of sinusoidal functions for the Set Membership data set, and a list of inclination targets (obtained through velocity feedback) for the Recursive least squares method. To compare both, the same input should be considered, therefore the second scheme with the feedback inclination was used for comparison.

Fig. 4 shows a fragment of the data sets used for identification. As you can see, the signal provides a wide frequency spectrum as desired.

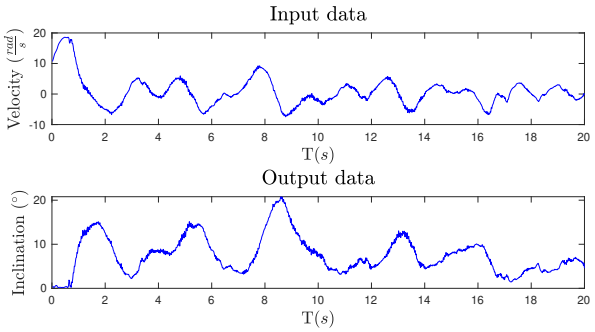

Fig. 4: Segment of input and output data sets used for system identification.

VI. Results and Discussion

In this section we present the SM behavior on the validation data compared to those obtained by a NLARX NN with 2 hidden layers and 25 neurons each. In addition, we include the resulting model for RLS with the forgetting factor. Finally, to validate the results, there are three different tests that compare the methodologies used.

A. SM results

SM results are shown in Fig. 5. The method follows the output throughout the validation set. The $NRMSE$ fit for the output reaches 88.75%, 5% lower than the neural network, but well above the 58% of the NLARX (NonLinear Auto-Regressive with eXogenous input) model of Matlab identification, with the same data sets. Both methods follow the system dynamics in frequency and magnitude.

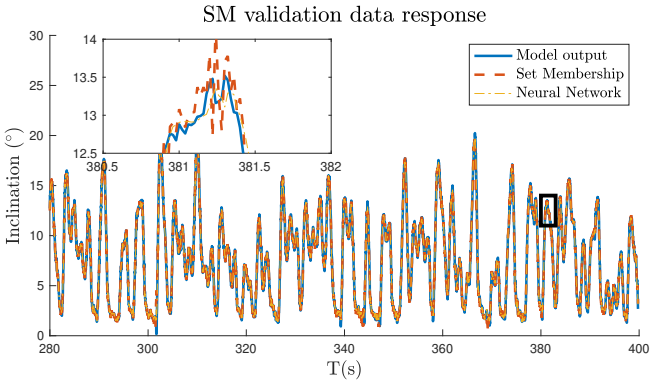

Fig. 5: Results for Set Membership and neural network for the validation data.

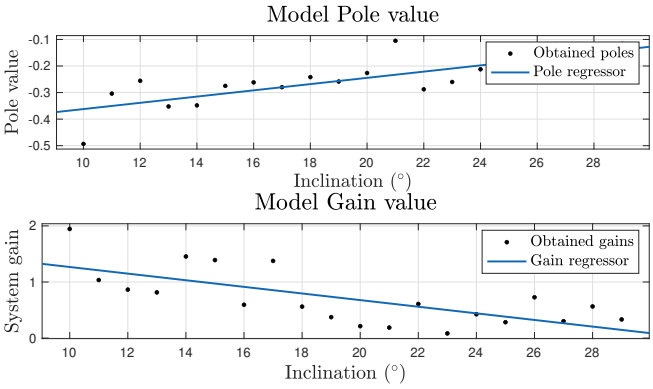

Fig. 6: Parameters obtained from online system identification for different neck inclinations.

B. RLS results

The plant has been modeled as first order, actuator velocity input, inclination velocity output, therefore, a pole and a gain are the system parameters. The results obtained by applying the RLS method in several experiments for different inclinations are shown in Fig. 6, where the poles (top) and gains (bottom) are plotted against the final inclination angle.

Note how the values of both the pole and the gain tend towards zero. Given the shape of the data, a linear approximation by least squares may be useful. The results of the least squares fitting of the data are as follows

- $N = -0.059 \cdot i + 1.857$
- $P = 0.01175 \cdot i - 0.4797$

where i variable represents the neck current inclination. Using those equations an inclination dependent transfer function is obtained. Equation (16) shows the final RLS model.

$$G_{rls}(z, i) = \frac{N}{z - P} \tag{16}$$

Once both models are available, a set of tests will show compared accuracy for both approaches.

C. Methods Comparison

To compare the performance of the methods, we used the prediction results. Next, a simulation of the neck is performed and compared to the actual neck output and to the Neural Network.

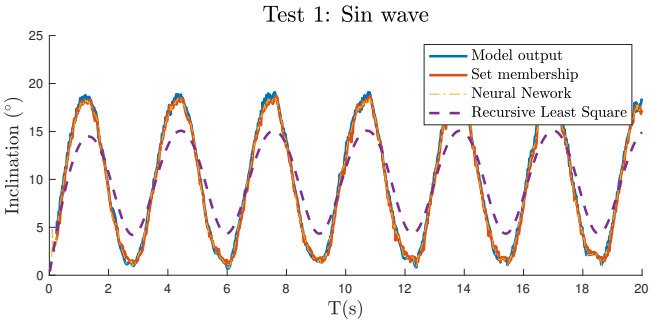

Fig. 7: Model comparison for a sin wave.

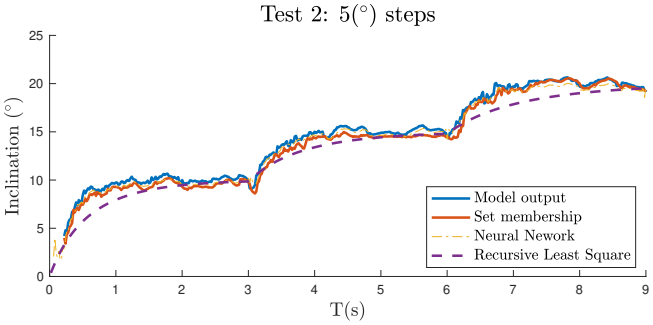

Fig. 8: Model comparison for a increasing step input.

1) Test 1: it consists of a constant sinusoidal wave input with 2 rad frequency to the close loop system. Fig. 7 shows how RLS follows the system response with similar trends to the real output, however it is much slower than the actual plant output, and does not reach the maximum and minimum system responses. In addition, the model follows the rising inclination which is governed by the actuator better than the lowering inclination, which is given by the spring return effect and the actuation mechanism. Meanwhile, both NN and SM follow the sin wave with a low error. The NN has, for $NRMSE$, a 92% fit; while SM follows with a 91% fit.

2) Test 2: for this test a 5 ° increasing step wave every 3 seconds is set as input. Fig. 8 shows how RLS results are close to the actual system output, but the setting time is slower. NN and SM again follow the real system dynamics with low error and high frequency response, and the elastic-plastic behavior is properly modeled. Their respective fits are 86.25% and 84.65%.

3) Test 3: The third an final test consists of a constant 20° step input to the system. Fig. 9 shows how the RLS follows the system response, but the setting time is slower than the actual plant. On the other hand, NN and SM responses follow the model output as desired. In this case, however, the error is greater than in previous tests. Their respective fits are 75.16% and 67.87%. Even though the fits are not as high as one might wish, the mean error is 0.39 ° for the SM.

VII. Conclusions

This paper presents a soft link characterization for control purposes, which results in two plant models, a nonlinear

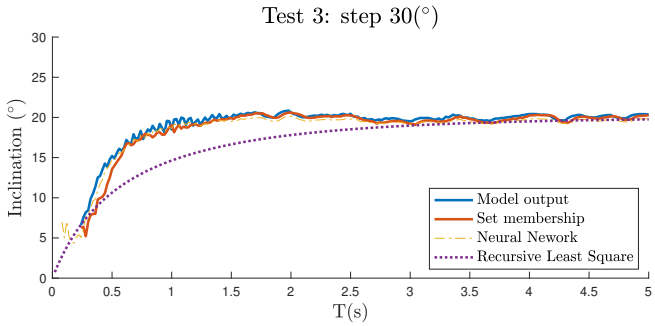

Fig. 9: Model comparison for a step input.

black box model from NN and SM identifications, and a linearized transfer function by parts from RLS methods.

All test results confirm that a correct model for the nonlinear dynamics of the neck was obtained. The SM model follows a behaviour close to all the real system outputs in the different experiments. When compared to NN, the results are very close, which makes Set Membership an excellent alternative to Neural networks. In this case, the models can be used for control and simulation purposes.

In the RLS with forgetting factor, the system dynamics was captured, but the frequency response is slower and the elastic-plastic characteristics of the system are not properly modeled. This might limit its use in certain applications, but future control applications are possible when working with low frequencies.

With our results, a well-designed control system is now possible. The identification results found are good enough for standard controller tuning purposes, and although it is beyond the scope of this paper, more advanced control schemes can be proposed from here, such as adaptive, predictive or robust controllers.

VIII. Aknowledgments

The research leading to these results has received funding from the HUMASOFT project, with reference DPI2016-75330-P, funded by the Spanish Ministry of Economyand Competitiveness, and from the RoboCity2030-DIH-CMMadrid Robotics Digital Innovation Hub (Robótica aplicada a la mejora de la calidad de vida de los ciudadanos, FaseIV; S2018/NMT-4331), funded by Programas de Actividades I+D en la Comunidad de Madrid and cofunded by Structural Funds of the EU.

References

[1] X. Chen, Y. Guo, D. Duanmu, J. Zhou, W. Zhang, and Z. Wang, "Design and modeling of an extensible soft robotic arm," *IEEE Robotics and Automation Letters*, vol. 4, no. 4, pp. 4208–4215, 2019.

[2] J. Wang, Y. Fei, and W. Pang, "Design, modeling, and testing of a soft pneumatic glove with segmented pneunets bending actuators," *IEEE/ASME Transactions on Mechatronics*, vol. 24, no. 3, pp. 990–1001, 2019.

[3] P. Polygerinos, Z. Wang, J. T. Overvelde, K. C. Galloway, R. J. Wood, K. Bertoldi, and C. J. Walsh, "Modeling of soft fiber-reinforced bending actuators," *IEEE Transactions on Robotics*, vol. 31, no. 3, pp. 778–789, 2015.

[4] A. Villoslada, C. Rivera, N. Escudero, F. Martín, D. Blanco, and L. Moreno, "Hand exo-muscular system for assisting astronauts during extravehicular activities," *Soft Robotics*, vol. 6, 11 2018.

[5] M. Xiloyannis, L. Cappello, D. B. Khanh, S.-C. Yen, and L. Masia, "Modelling and design of a synergy-based actuator for a tendon-driven soft robotic glove," in *2016 6th IEEE International Conference on Biomedical Robotics and Biomechatronics (BioRob)*. IEEE, 2016, pp. 1213–1219.

[6] C. J. Nycz, M. A. Delph, and G. S. Fischer, "Modeling and design of a tendon actuated soft robotic exoskeleton for hemiparetic upper limb rehabilitation," in *2015 37th Annual International Conference of the IEEE Engineering in Medicine and Biology Society (EMBC)*. IEEE, 2015, pp. 3889–3892.

[7] D. Rus and M. T. Tolley, "Design, fabrication and control of soft robots," *Nature*, vol. 521, no. 7553, pp. 467–475, 2015.

[8] Y. Long, Z. Du, L. Cong, W. Wang, Z. Zhang, and W. Dong, "Active disturbance rejection control based human gait tracking for lower extremity rehabilitation exoskeleton," *ISA transactions*, vol. 67, pp. 389–397, 2017.

[9] J. C. Cambera, J. A. Chocoteco, and V. Feliu-Batlle, "Modeling and identification of a single link flexible arm with a passive gravity compensation mechanism," in *2018 IEEE International Conference on Robotics and Automation (ICRA)*. IEEE, 2018, pp. 7704–7710.

[10] Z. Gong, Z. Xie, X. Yang, T. Wang, and L. Wen, "Design, fabrication and kinematic modeling of a 3d-motion soft robotic arm," in *2016 IEEE International Conference on Robotics and Biomimetics (ROBIO)*. IEEE, 2016, pp. 509–514.

[11] T. Wang, Y. Zhang, Z. Chen, and S. Zhu, "Parameter identification and model-based nonlinear robust control of fluidic soft bending actuators," *IEEE/ASME Transactions on Mechatronics*, vol. 24, pp. 1346–1355, 06 2019.

[12] L. Mena, C. A. Monje, L. Nagua, J. Muñoz, and C. Balaguer, "Sensorización de un sistema de eslabón blando actuando como cuello robótico," in *Actas de las Jornadas Nacionales de Robótica*. Universidad de Alicante, 06 2019, pp. 98–102.

[13] L. Nagua, C. Monje, J. Muñoz Yañez-Barnuevo, and C. Balaguer, "Design and performance validation of a cable-driven soft robotic neck," in *Actas de las Jornadas Nacionales de Robótica*. Universidad de Valladolid, 06 2018.

[14] P. Pierro, S. Martinez, A. Jardon, C. Monje, and C. Balaguer, "Teo: Full-size humanoid robot design powered by a fuel cell system," *An International Journal on Cybernetics and Systems*, vol. 43, no. 3, pp. 163 – 180, 2012.

[15] L. Nagua, J. Muñoz, C. A. Monje, and C. Balaguer, "A first approach to a proposal of a soft robotic link acting as a neck," in *Actas de las Jornadas de Automática*. Área de Ingeniería de Sistemas y Automática, Universidad de Extremadura, Sep 2018, pp. 522–529.

[16] M. Milanese and C. Novara, "Set membership identification of nonlinear systems," *Automatica*, vol. 40, no. 6, pp. 957 – 975, 2004.

[17] I. D. Landau, R. Lozano, M. M'Saad, and A. Karimi, *Parameter Adaptation Algorithms—Deterministic Environment*. London: Springer London, 2011, pp. 55–120.

[18] J. Castaño, F. Ruiz, and J. Régnier, "A fast approximation algorithm for set-membership system identification," *IFAC Proceedings Volumes*, vol. 44, no. 1, pp. 4410 – 4415, 2011, 18th IFAC World Congress.

[19] M. Canale, L. Fagiano, and M. Milanese, "Set membership approximation theory for fast implementation of model predictive control laws," *Automatica*, vol. 45, no. 1, pp. 45 – 54, 2009.

[20] J. Castano and F. Ruiz, "Set membership identification of an excimer lamp for fast simulation," *Control Engineering Practice*, vol. 21, no. 1, pp. 96 – 104, 2013.

[21] K. Åström and P. Eykhoff, "System identification—a survey," *Automatica*, vol. 7, no. 2, pp. 123 – 162, 1971.

[22] K. J. Åström, "Matching criteria for control and identification," in *European control conference*, vol. 3, 1993, pp. 248–251.

[23] R. Lozano and Xiao-Hui Zhao, "Adaptive pole placement without excitation probing signals," *IEEE Transactions on Automatic Control*, vol. 39, no. 1, pp. 47–58, Jan 1994.